



HAL
open science

Unstructured Grid Convergence Study

Ganbo Deng, Alban Leroyer, Emmanuel Guilmineau, P. Queutey, Michel Visonneau, J. Wackers

► **To cite this version:**

Ganbo Deng, Alban Leroyer, Emmanuel Guilmineau, P. Queutey, Michel Visonneau, et al.. Unstructured Grid Convergence Study. 5th Conference on Computational Mechanics, CCM 2016, Aug 2016, Xi'an, China. hal-02567256

HAL Id: hal-02567256

<https://hal.science/hal-02567256v1>

Submitted on 7 May 2020

HAL is a multi-disciplinary open access archive for the deposit and dissemination of scientific research documents, whether they are published or not. The documents may come from teaching and research institutions in France or abroad, or from public or private research centers.

L'archive ouverte pluridisciplinaire **HAL**, est destinée au dépôt et à la diffusion de documents scientifiques de niveau recherche, publiés ou non, émanant des établissements d'enseignement et de recherche français ou étrangers, des laboratoires publics ou privés.

UNSTRUCTURED GRID CONVERGENCE STUDY

G. Deng, A. Leroyer, E. Guilmineau, P. Queutey, M. Visonneau, J. Wackers
METHRIC, LHEEA/UMR 6598 CNRS, Ecole Centrale de Nantes, France

SUMMARY

This paper focus on convergence study of CFD prediction using unstructured grid with our in house finite volume unstructured RANSE solver ISIS-CFD. Computations have been performed with different grid sets generated with different approaches including similar grid generation with unstructured grid generator and adaptive grid refinement. Numerical uncertainty is evaluated with Richardson extrapolation. Results obtained both with wall function and wall resolved approach are compared. It demonstrates that adaptive grid refinement is the most reliable approach for obtaining a grid independent solution.

1 INTRODUCTION

As CFD simulation is playing an important role in design procedure, industrial users is paying more and more attention to the reliability of numerical prediction. The most common practice for industrial users is to adjust numerical setup (mesh density, physical model, numerical scheme, ...) and compare the numerical prediction with the measurement data. If the agreement is good enough, then, such setup will be used as guideline for applications under similar condition. Although such procedure can help user to obtain a good prediction, it cannot rigorously quantify the numerical uncertainty in a simulation. The recommended procedure to quantify numerical uncertainty is to perform a verification and validation exercise. There are three kinds of verification and validation exercises, namely code verification, solution verification and solution validation. Code verification aims at demonstrating that the governing equations are solved correctly. The most appropriate approach for this exercise is to modify the code by adding source terms such that numerical solution can be compared with a manufactured solution. With the manufactured solution, one can easily verify the order of convergence of the flow solver as the mesh is refined. If the observed order of convergence agrees with the expected theoretical order of convergence as the mesh is refined, numerical implementation is considered as successful. Such code verification exercise can be done only once during the code development and does not need to be repeated for practical application. Unlike code verification, solution validation needs to be performed for every time if rigorous uncertainty quantification is required. It aims at quantifying errors due to numerical approach. Different sources of error exist in a numerical simulation. The most commons are space and time discretization error, convergence error, errors due to boundary condition and computational domain, etc. We focus to error due to spatial discretization only in this paper. The most common and the most reliable approach to access spatial discretization error is to perform simulation on a set of similar grid, then apply an uncertainty

estimation based on Richardson extrapolation. The success of such uncertainty estimation procedure depends on how such similar grid set is generated. Generating a similar grid set with structured grid is a trivial task. Unfortunately, industrial applications are commonly performed with unstructured grid. Ensuring grid similarity when generating a set of unstructured grid is nearly impossible. The situation is worse when wall function approach is used. Wackers and al. [3] have proposed an alternative to generate a set of similar grid for uncertainty estimation with adaptive grid refinement controlled by grid refinement threshold. This approach has been successfully applied to an uncertainty estimation exercise for a simple 2D airfoil configuration as well as a more complex 3D ship flow test case both for global quantities (resistance) and for local quantities (velocity). The objective of this paper is to compare the approach proposed by Wackers et al. with a more classical grid generation approach using grid generator in the uncertainty estimation exercise. Computation will be performed both with wall function and with wall resolved approach with a very simple 2D configuration for which structured grid set can also be generated for comparison.

2 NUMERICAL APPROACH

Computation has been performed with the ISIS-CFD flow solver developed by our team. Turbulent flow is simulated by solving the incompressible Reynolds-averaged Navier-Stokes equations (RANS). The flow solver is based on finite volume method to build the spatial discretization of the transport equations. The velocity field is obtained from the momentum conservation equations and the pressure field is extracted from the mass conservation constraint, or continuity equation, transformed into a pressure-equation. In the case of turbulent flows, additional transport equations for modeled variables are discretized and solved using the same principles. The gradients are computed with an approach based on Gauss's theorem.

Non-orthogonal correction is applied to ensure a formal first order accuracy. Second order accurate result can be obtained on a nearly symmetric stencil. Inviscid flux is computed with a piecewise linear reconstruction associated with an upwinding stabilizing procedure which ensures a second order formal accuracy when flux limiter is not applied. Viscous flux are computed with a central difference scheme which guarantee a first order formal accuracy. We have to rely on mesh quality to obtain a second order discretization for the viscous term. Free-surface flow is simulated with a multiphase flow approach. Incompressible and non-miscible flow phases are modeled through the use of conservation equations for each volume fraction of phase/fluid. Implicit scheme is applied for time discretization. Second order three-level time scheme is employed for time-accurate unsteady computation. Velocity-pressure coupling is handled with a SIMPLE like approach. Ship free motion can be simulated with a 6 DOF module. Some degree of freedom can be fixed as well. An analytical weighting mesh deformation approach is employed when free-body motion is simulated. Overset approach is implemented recently. It will be employed in one of the test cases in the present study. Several turbulence models ranging from one-equation model to Reynolds stress transport model are implemented in ISIS-CFD. Most of the classical linear eddy-viscosity based closures like the Spalart-Allmaras one-equation model, the two-equation $k-\omega$ SST model by Menter [2], for instance are implemented. A more sophisticated turbulence closures are also implemented in the ISIS-CFD solver, an explicit algebraic stress model (EASM) [1]. The EASM model is employed in the present study. Wall function is implemented for two-equation turbulence model.

Adaptive grid refinement is implemented in the ISIS-CFD flow solver with different refinement criterion. In the present study, we aim at resistance prediction only. To this end, the best refinement criterion is the pressure Hessian which is a tensor based on the second derivatives of the pressure field. In the refinement procedure, the mesh is refined until the module of a vector resulting from the tensor product between the cell size vector and the pressure Hessian tensor is smaller than a threshold value. Details can be found in [4].

3 SIMILAR MESH SET GENERATION

The success of an uncertainty estimation exercise depends strongly how the mesh set employed for the computation is generated. Richardson extrapolation can give the expected result only when grid similarity of the mesh set is ensured. Two grids are considered as similar when mesh orientation at the same position is the same, and the mesh size ratio between the two grids at any location is a constant. When using wall function, grid similarity can no longer be ensured in the near wall region, since the cell size in the

wall normal direction should be kept unchanged. We employ the hexahedral unstructured grid generator Hexpress for mesh generation. With Hexpress, it is not possible to ensure grid similarity everywhere. Figure 1 shows two meshes with a refinement ratio of 2 generated with Hexpress. Although the mesh size ratio is about 2 everywhere, the location of grid refinement interface is not exactly the same. The most annoying drawback of the mesh generator Hexpress is that the boundary layer thickness becomes smaller in the fine grid. Hence, in a convergence study using Hexpress, adding more fine grid usually can not help to obtain a better convergence behavior.

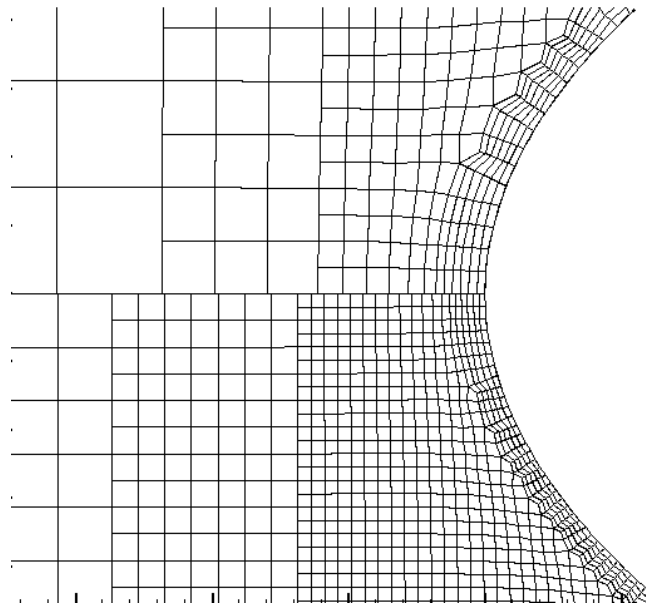


Figure 1. Unstructured grid generated with Hexpress

An alternative to generate a similar grid set is to perform an adaptive grid refinement by using different refinement threshold. Figure 2 displays two meshes issued from grid adaptation. Pressure Hessian is employed as refinement criterion in this computation. The upper part is the coarse mesh, while the lower part is the fine mesh. The ratio for the refinement threshold is equal to 2. It can be seen that mesh size ratio is equal to 2 all most everywhere except in the boundary layer where we intentionally refine the mesh in the wall tangential direction only in order to preserve mesh quality in the viscous layers. The refined mesh is projected automatically to the surface of the real geometry. As the initial mesh is relatively coarse, the thickness of viscous layer of the refined grid is much bigger compared to the mesh generated directly with the mesh generator Hexpress shown in figure 1. Moreover, it remains constant whatever the degree of grid refinement. Hence, turbulence boundary layer can be better captured when using adaptive grid refinement. It should be noticed that the distance to the wall for the first grid cell is specified with the same value corresponding to about $y^+=30$ when generating the grid. The different cell size observed in figures 1 and 2 are the result of mesh optimization performed by the mesh generator.

Meshes shown in figures 1 and 2 are designed for wall function computation. When generating grid set for wall resolved computation with mesh generator, it is possible to adjust the distance to the wall for the first grid cell such that grid similarity is also ensured in the near wall region. However, as refinement will not be applied in the wall normal direction, grid similarity near the wall is impossible to ensure with adaptive grid refinement. Hence, we decide to generate a grid set with the same distance to the wall corresponding to about $y^+=0.2$ when using grid generator approach.

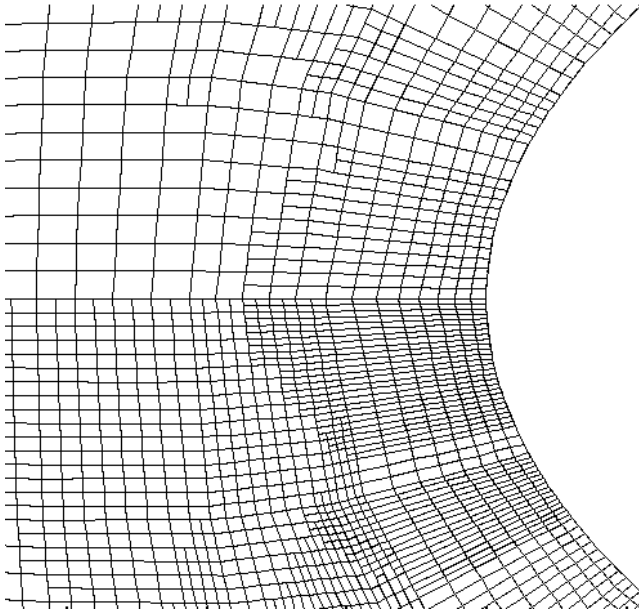


Figure 2. Mesh obtained with adaptive grid refinement

4 CONVERGENCE STUDY RESULTS

The test case investigated in the present paper is a simple ellipse geometry with an aspect ratio of 1:5 in two dimension. The computational domain is defined by $-6L < x < 18L$, $-4L < y < 4L$, L being the chord of the ellipse. The center of the ellipse is located at $(0,0)$. The pressure is set to 0 at the outlet boundary $x=18L$, while far field boundary condition with constant velocity is imposed at the remaining outer boundaries. Reynolds number based on the chord length is $1.0e6$.

Index	Threshold	N	Fxp	Fx
1	0.36	16114	0.004324	0.009366
2	0.24	31577	0.004244	0.009289
3	0.18	52291	0.004208	0.009256
4	0.12	121853	0.004198	0.009248
p	-	-	2.21	2.35
U_e	-	-	0.004183	0.009236
U_{e2}	-	-	0.004177	0.009228

Table 1: Wall modeled prediction with adaptive refinement

Table 1 presents the results obtained with adaptive grid refinement. N is the number of grid cells. F_{xp} is the pressure resistance, while F_x is the total resistance. Both are normalized values using chord length and far field velocity. “p” is the observed order of convergence. U_e is the extrapolated result with observed order of convergence, while U_{e2} is the extrapolated value obtained with assumed second order accuracy of the finite volume flow solver. As the mesh in the wall normal direction is not refined, it is expected that monotonic convergence behavior can not be obtained for friction resistance. For this reason, it is not shown in the table. For the computation with adaptive refinement, extrapolation is performed with respect to the threshold value. The observed order of convergence is not too far from the expected second order accuracy both for pressure resistance and for the total resistance. This indicates that the grid convergence study is successful. Prediction obtained with the finest grid differs from the extrapolated solution U_{e2} by about 0.5% and 0.2% for pressure resistance and total resistance respectively. Based on the extrapolated value U_{e2} for pressure resistance and total resistance, the expected friction resistance is 0.005051.

Index	N1	N	100Fxp	100F _{xv}	100F _x
1	72	11040	0.3897	0.5046	0.8943
2	96	18484	0.3248	0.5128	0.8276
3	120	27448	0.3252	0.5126	0.8379
4	144	40806	0.3502	0.5198	0.8600
5	168	55134	0.3509	0.5182	0.8690
6	192	72186	0.3620	0.5173	0.8793
7	216	90420	0.3683	0.5149	0.8837
8	240	109988	0.3780	0.5148	0.8928
9	264	136070	0.4367	0.5175	0.9542

Table 2: Wall modeled prediction with mesh generation

Table 2 shows the predicted pressure resistance F_{xp} , friction resistance F_{xv} and the total resistance F_x . $N1$ is the number of mesh point in the X direction of the initial mesh generated by Hexpress. $1/N1$ can be used as mesh size for the Richardson extrapolation. With $N1=72$, the coarsest grid contains 3 cells in the initial mesh. The initial mesh is refined by 5 levels in Hexpress, resulting 96 cells per chord length. One more level of refinement is applied near the leading edge and the trailing edge. Mesh size is about $L/192$ in those regions. The first grid is too coarse. Starting from grid 2 until grid 8, predicted pressure resistance and total resistance increase monotonously and approach the expected solution given in table 1. However, even on grid 8, pressure resistance is still 9.5% smaller than the extrapolated solution U_{e2} given in table 1, while the total resistance is 3.3% smaller. Further refinement with grid 9 does not allow to improve the prediction. The predicted result becomes much bigger than the expected value suddenly. Inspection of the numerical solution reveals that this sudden change in convergence behavior in grid 9 is due to the fact that the thickness of viscous layer becomes too small. Cells with poor quality in the transition region

between the viscous layer and the outer layer deteriorate the accuracy of numerical prediction in the viscous layer. Results shown in table 2 show the limitation with grid generation approach when using the unstructured grid generator.

Analysis of the predicted numerical solution reveals that the poor convergence behavior shown in table 2 is due to the fact that grid density near the trailing edge is not sufficient. In fact, a small recirculation zone is formed in this region. Higher grid resolution is required in this region in order to capture the flow separation correctly. We regenerate a new grid set by increasing one more refinement level both in the leading edge and the trailing edge. On the coarsest grid 1, mesh size is $L/394$ in those regions.

Index	N1	N	100Fxp	100F xv	100Fx
1	72	13010	0.3822	0.5092	0.8915
2	96	21510	0.3780	0.5077	0.8857
3	120*	31730	0.3803	0.5045	0.8926
4	144*	46794	0.3945	0.5041	0.8987
5	168*	63060	0.3967	0.5075	0.9043
6	192*	82458	0.4036	0.5055	0.9091
7	216*	103266	0.4061	0.5064	0.9125
p	-	-	2.50	2.37	0.14
U_e	-	-	0.4131	0.5072	1.1428
U_{e2}	-	-	0.4173	0.5074	0.9201

Table 3: Wall modeled prediction with mesh generation

Table 3 shows the predicted resistance as well as the extrapolated solution. The first two grids are too coarse. The extrapolated is obtained with the last 5 finest solutions marked by a * in the table. For the pressure resistance, the observed order of convergence is 2.50. The extrapolated solution $U_{e2} = 0.4173$ differs from the corresponding result obtained with adaptive grid refinement shown in table 1 by less than 0.1%. This good agreement suggests that the prediction with grid generation approach is successful this time. However, it should be noticed that on the finest grid 7, the predicted pressure resistance is still 2.7% smaller than the expected value, while with adaptive grid refinement, prediction obtained with grid 4 with similar number of grid cells is only 0.5% smaller than U_{e2} . For this computation, monotonic convergence behavior is also observed for the friction resistance with an observed order of convergence of 2.37. However, the predicted solutions do not change monotonously. Hence, this extrapolated result cannot be considered as reliable. Due to the poor convergence behavior in friction resistance, the observed order of convergence for the total resistance $p=0.14$ is too small. In this case, only the extrapolated solution with assumed second order accuracy U_{e2} can be used for uncertainty estimation. This extrapolated value differs from the value shown in table 1 by 0.3%. This good agreement confirm once again the good convergence behavior obtained with this grid set. On the finest grid 7,

the predicted total resistance is 0.8% smaller than the extrapolated solution U_{e2} .

The adaptive grid refinement approach is applied for wall resolved computation. Results are shown in table 4. Monotonic convergence behavior is observed for all resistance components with an observed order of convergence higher than 3. This high value of observed order of convergence may due to the fact that in our computation, grid is not refined in the wall normal direction. Hence, grid similarity is not ensured. The predicted pressure resistance and total resistance are 0.53% and 0.26% higher than the extrapolated solution U_{e2} respectively, similar to what we obtained in the computation with wall modeled computation shown in table 1.

Index	Threshold	N	100Fxp	100F xv	100Fx
1	0.36	32291	0.4507	0.4847	0.9354
2	0.24	55133	0.4421	0.4843	0.9264
3	0.18	82545	0.4401	0.4843	0.9244
4	0.12	179286	0.4393	0.4842	0.9235
p	-	-	3.15	3.28	3.18
U_e	-	-	0.4388	0.4824	0.9230
U_{e2}	-	-	0.4370	0.4841	0.9211

Table 4: Wall resolved prediction with adaptive refinement

Index	N1	N	100Fxp	100F xv	100Fx
1	72	24260	0.3851	0.4902	0.8753
2	96	36360	0.3751	0.4907	0.8659
3	120*	50330	0.3783	0.4910	0.8693
4	144*	68346	0.3966	0.4908	0.8873
5	168*	87026	0.4100	0.4892	0.8991
6	192	108638	0.4274	0.4863	0.9136
7	216	131280	0.4406	0.4835	0.9242
p	-	-	0.84	-	1.51
U_e	-	-	0.5068	-	0.9440
U_{e2}	-	-	0.4421	0.4877	0.9298

Table 5: Wall resolved prediction with mesh generation

Table 5 shows the results obtained with wall resolved simulation using grid set generated by mesh generator Hexpress. Poor convergence behavior similar to the result shown in table 2 is observed. The predicted pressure and total resistance are smaller than the expected value. They increase as the grid is refined. But on the finest grid 7, the predicted pressure resistance and total resistance become larger than the expected value U_{e2} shown in table 4. Again, this poor convergence behavior is due to the fact that grid similarity is not ensured in the near wall region with mesh generation approach. Moreover, poor quality cells next to the viscous layer deteriorate the accuracy of numerical prediction in the viscous layer. It is very difficult to obtain a reliable uncertainty estimation for this simulation.

Extrapolated results shown in table 5 are obtained with a selected grid triplets marked with a * in the table. The extrapolated U_{e2} values differ from the results obtained with adaptive grid refinement given in table 4 by about 1% for all resistance components. But this extrapolation can not be considered as reliable.

5 CONCLUSIONS

Grid convergence study for unstructured grid is investigated with different approaches using a simple 2D geometry. The newly proposed grid adaptive refinement approach is found to be capable to provide a solution with good convergence behavior both for wall modeled and for wall resolved simulation. With grid generation approach, as unstructured grid generator is unable to generate a grid set ensuring grid similarity everywhere, user expertise is required when generating the grid. If the grid is well adapted to the flow, a good convergence behavior can be obtained. On the other hand, a poor convergence behavior is always an indication that the numerical prediction is not reliable. Such poor convergence behavior may be due to a too coarse grid resolution, or a poor grid quality locally. Generating a still finer grid cannot always improve the prediction. Compared with usual approach by generating grid set with grid generator, adaptive grid refinement approach is found to be more reliable way to generate similar grid set employed in a verification and validation exercise.

6 ACKNOWLEDGEMENTS

This work was granted access to the HPC resources under the allocation 2015-2a1308 made by GENCI (Grand Equipement National de Calcul Intensif).

7 REFERENCES

1. G.B. Deng, P. Queutey and M. Visonneau. (2005). Three-Dimensional Flow Computation with Reynolds Stress and Algebraic Stress Models. *Engineering Turbulence Modelling and Experiments 6*, W. Rodi and M. Mulas eds. ELSEVIER, pp. 389-398..
2. F.R. Menter. (1993). Zonal two-equations $k-\omega$ turbulence models for aerodynamic flows. *AIAA Paper* 93-2906.
3. J. Wackers, G. Deng, E. Guilmineau, A. Leroyer, P. Queutey, M. Visonneau, A. Palmieri, & A. Liverani, (2016). Can adaptive grid refinement produce grid-independent flow solutions? Submitted to *Journal Computational Physic*.
4. J. Wackers, G. Deng, E. Guilmineau, A. Leroyer, P. Queutey, M. Visonneau, (2014). Combined refinement criteria for anisotropic grid refinement in free-surface flow simulation, *Comput Fluids* 92, pp 209-222.